Wiley
Nanomaterials and Nanotechnology
Volume 2025, Article ID 5594031, 13 pages
https://doi.org/10.1155/nax2/5594031

Research Article

Biosynthesis of Zinc Oxide Nanoparticles Using Aqueous Leaf Extract of *Alternanthera philoxeroides* for Antioxidant and Antibacterial Activities

Ruchika Sharma,[1] Sheetal Tyagi,[1] Rakesh Kumar Bachheti,[2] Archana Bachheti,[3] and Limenew Abate Worku[4]

[1]*Department of Chemistry, School of Basic and Applied Sciences, Shri Guru Ram Rai University, Dehradun, Uttarakhand, India*
[2]*Centre of Molecular Medicine and Diagnostics, Saveetha Dental College & Hospitals, Saveetha Institute of Medical and Technical Sciences, Saveetha University, Chennai, India*
[3]*Department of Environment Science, Graphic Era (Deemed to be University), Dehradun 248002, Uttarakhand, India*
[4]*Departments of Chemistry, College of Natural and Computational Science, Debre Tabor University, Debre Tabor, Ethiopia*

Correspondence should be addressed to Sheetal Tyagi; sheetalty@gmail.com and Limenew Abate Worku; limenewabate@gmail.com

Received 24 May 2025; Revised 10 November 2025; Accepted 20 November 2025

Academic Editor: Raphael Schneider

Copyright © 2025 Ruchika Sharma et al. Nanomaterials and Nanotechnology published by John Wiley & Sons Ltd. This is an open access article under the terms of the Creative Commons Attribution License, which permits use, distribution and reproduction in any medium, provided the original work is properly cited.

In the contemporary scientific landscape, the demand for sustainable and nontoxic synthesis of metallic nanoparticles has grown significantly, with biological or green synthesis approaches being preferred over conventional physical and chemical methods due to their eco-friendly, cost-effective, and nonhazardous nature. In this study, zinc oxide nanoparticles (ZnONPs) were synthesized via a simple and environmentally benign process using an aqueous leaf extract of *Alternanthera philoxeroides* as a natural bio-reducing and stabilizing agent, along with zinc acetate as the precursor salt. The formation of *A. philoxeroides*–mediated ZnONPs was confirmed by a characteristic surface plasmon resonance (SPR) band at 351 nm in the ultraviolet-visible (UV-Vis) spectrum and by energy dispersive X-ray (EDX) analysis showing elemental zinc and oxygen. Fourier transform infrared (FTIR) spectroscopy displayed peaks at 3,397, 2,930, 1,633, 1,408, 1,312, 1,072, 1,025, 821, and 619 cm^{-1}, indicating phytochemicals responsible for reduction and capping. Zeta potential analysis yielded a value of −16.4 mV, reflecting moderate stability. X-ray diffraction (XRD) confirmed the crystalline wurtzite structure, further supported by the selected area electron diffraction (SAED) pattern. Field emission scanning electron microscopy (FESEM) revealed spherical nanoparticles with an average size of 15 nm, and high-resolution transmission electron microscopy (HRTEM) showed a size distribution between 3 and 35 nm with distinct lattice fringes. Antibacterial evaluation using the agar well diffusion method demonstrated the highest inhibition against *Staphylococcus aureus,* while antioxidant activity assessed by the 2,2-diphenyl-1-picrylhydrazyl (DPPH) free radical scavenging assay exhibited a half-maximal inhibitory concentration (IC_{50}) of 85.42 μg per milliliter (μg/mL), indicating strong radical neutralization capacity. These results highlight the potential of bio-synthesized ZnONPs for diverse biomedical, pharmaceutical, and industrial applications, warranting further investigation into their cytotoxicity, targeted drug delivery potential, and performance in real-world biomedical systems.

Keywords: *Alternanthera philoxeroides*; antibacterial activity; antioxidant activities; zinc oxide nanoparticle

1. Introduction

The term "nanotechnology" originates from the nanoscale range, referring to particles measuring between 1 and 100 nm [1]. In recent times, metallic nanoparticles have commonly been prepared using various physical and chemical methods. However, these techniques often involve toxic chemicals, which pose threats to human health and the environment. Moreover, they are often expensive, complex, and time-consuming. As a result, green chemistry has encouraged the search for safer alternatives, with biological methods emerging as a preferred route for sustainable nanoparticle production [2–4]. These biological methods follow green chemistry principles and make use of bacteria and fungi to synthesize nanoparticles in an environmentally friendly manner [5, 6]. Among the various biological approaches, the use of plant extracts has proven to be the safest, most cost-effective, and eco-friendly method for nanoparticle synthesis. This approach offers a simple and efficient way to produce high-yield and pure materials. Additionally, the phytochemicals naturally present in plant extracts assist in reducing metal ions and stabilizing the nanoparticles, thus removing the need for external reducing, capping, or stabilizing agents [7–9]. Traditionally, whole plants or leaf were used for metallic nanoparticle synthesis. However, recent advancements have enabled the use of extracts from flowers, seeds, fruits, roots, peels, and bark [10–12].

Zinc oxide nanoparticles (ZnONPs) stand out from other nanomaterials due to their unique chemical and optical properties. Structurally, they exhibit a wurtzite ZnO crystal structure, often forming cylindrical shapes with droplet-like nanoparticle at their tips, as observed in vapor liquid solid growth mechanism [13]. As a type of metal oxide, they demonstrate special catalytic and oxidative characteristics, making them ideal for various biotechnology and biomedical applications [11]. ZnONPs are widely used in diverse fields, including biology, cosmetics, pharmaceuticals, animal feed, medicine, environmental protection, coatings, rubber production, communication, sensors, and electronics. Studies have shown that differences in ZnONPs' size influence their properties, enhancing their versatility. The diameter distribution of ZnONPs mimics that of stabilizing nanoparticles formed during synthesis with nanoscale processes such as Ostwald ripening and/or coalescence occurring before final nanoparticle formation [13]. In addition, their nontoxic nature has led to growing applications in cosmetics, diagnostics, and textile industries [14–16]. ZnONPs are considered safe and exhibit strong antimicrobial properties, making them suitable for treating various infectious diseases in humans and animals. This distinguishes them from other metals commonly used in nanoparticle synthesis for clinical purposes. ZnONPs are used for doping the ZnO structure to improve their functionality [17].

Medicinal plants have been found in the Himalayan Mountain range since ancient times. People living in these areas have been using them for years to cure diseases [18, 19]. *Alternanthera philoxeroides, Artemisia roxburghiana, Leucas lantana,* and *Vinca major* are being used by us to make metallic nanoparticles.

In this study, we synthesized ZnONPs using leaf from *A. philoxeroides*, commonly referred to as alligator weed. This perennial, nonwoody aquatic plant belongs to the Amaranthaceae family and is native to South America, where it has become an invasive species in India. Researchers reported that the extract of the *A. philoxeroides* leaf is traditionally used to treat ailments such as dysentery, asthma, and stomachache. It contains alkaloids, amino acids, steroids, tannins, flavonoids, proteins, carbohydrates, and phenolic compounds, making it well-suited for the formation of metallic nanoparticles [20, 21]. The synthesis process involves vapor pressure changes during reduction leading to axial and radical growth of nanoparticle in a manner analogous to vapor solid mechanism resulting in well aligned nanostructure [13]. The novelty of this study lies in the fact that, to the best of our knowledge, the green synthesis of ZnONPs using *A. philoxeroides* has not been previously reported. This work highlights the potential of the *A. philoxeroides* leaf as a sustainable and eco-friendly source for nanoparticle fabrication.

2. Methods and Methodology

2.1. Plant Sample Collection. Leaves of *A. philoxeroides* were collected from the vicinity of Garg (P.G.) College, located in Laksar, Haridwar, Uttarakhand. The collection process was conducted in full compliance with the existing institutional, national, and international guidelines and regulations. The plant material was taxonomically identified and officially authenticated by the Botanical Survey of India, Dehradun. All procedures related to plant collection were strictly followed by national standards and ethical recommendations. A voucher specimen of the collected plant was submitted to the National Herbarium and was assigned the specimen number 1168.

2.2. Plant Extract Preparation. Fresh leaves of *A. philoxeroides* were thoroughly washed 2-3 times using tap water, followed by a final rinse with distilled water to eliminate dust and surface impurities. The cleaned leaves were then left to air dry in the shade at room temperature for 15–20 days during the month of October. Once thoroughly dried, they were ground into a fine powder. For the preparation of the aqueous extract, 20 g of the powdered material were mixed with 500 mL of distilled water and heated at 60°C for 20 min. The mixture was then filtered using Whatman No. 1 filter paper, and the resulting extract was stored at 4°C for further use [22–24].

2.3. Green Synthesis of ZnONPs. A total of 60 mL of the stored *A. philoxeroides* extract was transferred into a 250-mL conical flask and heated on a magnetic stirrer at 70°C for 15 min. While maintaining the same temperature and continuous stirring, a 20-mM zinc acetate solution was added dropwise to the extract. Subsequently, the pH of the reaction mixture was adjusted using an aqueous NaOH solution. The formation of ZnONPs was indicated by the appearance of turbidity in the solution. The resulting

precipitate was collected by centrifugation at 4000 rpm for 10 min and dried in a hot air oven at 70°C. The dried ZnONPs were then stored in an airtight container for future applications [25, 26].

2.4. Details of Characterization Techniques for ZnONPs. Using a JASCO V-650 ultraviolet-visible (UV-Vis) spectrophotometer, which records spectra in a wavelength range of 300–600 nm, the UV-Vis absorbance of the produced ZnONPs in ultrapure water was examined. ZnONP synthesis was first validated by the absorbance peak seen in the 300–400-nm region. A Nicolet 6700 spectrometer from Thermo Fisher Scientific, Germany, was also used to perform Fourier transform infrared (FTIR) spectroscopy on the ZnONPs in the 4000–400 cm^{-1} range. The nanoparticle compositional percentages and elemental purity were assessed using energy-dispersive X-ray (EDX) spectroscopy. Using a Bruker D8 Advance equipment (Germany) at room temperature, X-ray diffraction (XRD) was used to evaluate the ZnONP phase composition and structural analysis. CuKα radiation ($\lambda = 1.5406$ Å) was used for the measurements, which had a scattering angle range of 10°–80° and a step size of 0.02°. Using a Carl Zeiss Ultra Plus microscope in secondary electron mode and field emission scanning electron microscopy (FESEM), the surface microstructure and grain size of the nanoparticles were investigated. EDX spectroscopy was used with the FESEM to analyze the materials' chemical composition. The diameter and shape of the produced ZnONPs were assessed using high-resolution transmission electron microscopy (HRTEM) using Image J software (Version 1.52 v) developed by Wayne Rasband at the National Institutes of Health, USA. First, HRTEM of the ZnONPs were obtained. These images were then opened in ImageJ, and the software was calibrated by setting the scale using a known distance from the image's scale bar. After converting the image to 8-bit grayscale, the threshold was adjusted to clearly distinguish the nanoparticles from the background. The individual nanoparticles were then analyzed using the "Analyze Particles" tool, which provided measurements including the diameter. This method enabled accurate estimation of nanoparticle size distribution based on the image data. The sample was diluted in ethanol for this analysis, and a drop of the mixture was put onto a staining mat. After that, a copper grid coated with Lacey carbon was placed on the drop, coated side up. The grid was subjected to sonication for 30 min and then allowed to air dry for an additional 30 min before being analyzed using a JEOL 2100 transmission electron microscope. Finally, the nanoparticles' surface charge and particle size distribution were assessed using a Horiba Scientific SZ-100 device [27, 28].

2.5. Antioxidant Properties. The antioxidant activity of the biosynthesized ZnONPs was assessed using the 2,2-diphenyl-1-picrylhydrazyl (DPPH) free radical scavenging assay. DPPH is a stable free radical commonly employed to evaluate the radical-scavenging ability of antioxidants. In its methanolic solution, DPPH exhibits a deep violet color with a characteristic absorbance peak at 517 nm in the UV-Vis spectrum. Upon interaction with an antioxidant, DPPH undergoes reduction by accepting an electron, leading to a color change from violet to yellow due to decreased absorbance. In this assay, equal volumes of *A. philoxeroides leaf* extract or various concentrations of ZnONPs were mixed with 1 mL of DPPH solution prepared in ethanol and incubated at room temperature for 30 min. Ascorbic acid was used as the standard reference antioxidant. For the control, 1 mL of methanol was substituted in place of the extract or nanoparticles to determine the baseline absorbance [29, 30].

2.6. Antibacterial Activity. The antibacterial activity of the biosynthesized ZnONPs was evaluated using the agar well diffusion method against *Salmonella abony, Bacillus subtilis, Escherichia coli,* and *Staphylococcus aureus.* A sterile glass spreader was used to evenly distribute the bacterial inoculum over the surface of the nutrient agar plates. Once the agar had solidified, wells were created and filled with varying concentrations of biosynthesized ZnONP solutions. The plates were then incubated at 37°C for 24 h to allow bacterial growth and observe the development of inhibition zones. Different concentrations of leaf extracts and synthesized ZnONPs were prepared using 100% DMSO. Each concentration was tested in triplicate to ensure the reliability of the antibacterial assessment. The diameters of the inhibition zones were measured in millimeters and compared with the control to determine antibacterial effectiveness. Streptomycin was (10 μg/mL) served as the positive control for reference [31].

3. Results and Discussion

3.1. UV-Vis Spectroscopy. Noble metal nanoparticles are known for their unique optical properties, primarily attributed to surface plasmon resonance (SPR). According to Mie's theory, the presence of a single SPR band in the UV-Vis spectrum typically signifies the formation of spherical nanoparticles. In contrast, anisotropic nanoparticles display multiple SPR bands due to variations in shape. In the present study, the UV-Vis spectral analysis of biosynthesized ZnONPs at room temperature revealed a distinct and sharp SPR peak at 351 nm, as shown in Figure 1, confirming the successful synthesis of ZnONPs. The sharpness and position of this peak strongly support the formation of well-dispersed, nanoscale ZnO particles. These findings are in agreement with previous studies, where ZnONPs synthesized using *Atalantia monophylla* and *Aloe barbadensis* miller leaf extracts also exhibited characteristic absorption in a similar range [32–34]. The consistency in absorption wavelength across different plant-mediated syntheses suggests that plant phytochemicals play a crucial role in stabilizing and controlling the size and morphology of ZnONPs. Moreover, the narrowness of the observed peak implies a uniform particle size distribution, which is often critical for applications requiring optical and biological consistency.

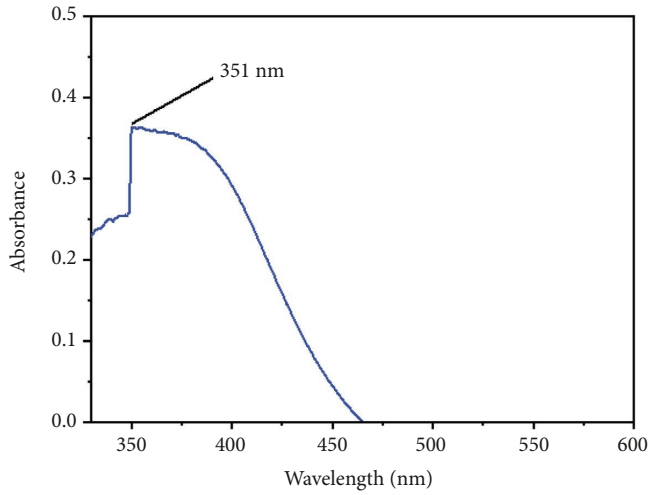


Figure 1: UV-Vis spectra for biosynthesized ZnONPs.

3.2. XRD. Figure 2 shows the XRD pattern of ZnONPs synthesized using *A. philoxeroides*, with diffraction peaks at 34, 36, 47, 56, and 67°, corresponding to planes [002], [101], [102], [110], and [112], confirming a hexagonal wurtzite structure (JCPDS No. 00-001-1136). Additional minor peaks near 26° suggest the presence of crystallized phytochemicals acting as capping agents. This is further supported by the FTIR analysis, indicating the role of bioactive compounds in nanoparticle stabilization. The sharp, well-defined peaks also highlight the high crystallinity and purity of the biosynthesized ZnONPs [21, 35–37].

3.3. EDX Analysis and Elemental Mapping. EDX analysis was conducted to determine the purity, elemental composition, and stoichiometry of the synthesized ZnONPs. The Zn content was 33.5%, while oxygen and carbon content were 25.5% and 44.1% as shown in Figure 3(a). In EDX of biosynthesized ZnONPs, single peak for Zn and oxygen between 2 and 3 keV and two peaks between 8 and 10 keV were obtained for Zn. The presence of a high percentage of carbon confirms the role of phytochemicals in the capping of the biosynthesized ZnONPs, which FTIR also confirmed. As shown in Figure 3 (b), we have performed element mapping of elements. This digital image illustrates the spatial distribution of elements present in the biosynthesized ZnONPs. From the element mapping image, a homogenous distribution of the Zn, O, and C is clearly noticeable [37–39].

3.4. FESEM Analysis. The surface morphology of the biosynthesized ZnONPs was examined using FESEM, which revealed white, densely packed, and predominantly spherical nanoparticles, as illustrated in Figure 4(a). These observations were further corroborated by HRTEM imaging. The observed nanoparticle aggregation can be attributed to van der Waals forces and magnetic interactions among ZnONPs. EDX analysis confirmed the elemental purity of the synthesized nanoparticles. ImageJ software was employed to estimate particle size, analyzing 61 individuals' ZnONPs, yielding an average size of approximately 15 nm (Figure 4(b)). These results were consistent with XRD and HRTEM findings, supporting the formation of uniform, crystalline ZnONPs. The uniformity in size and shape suggests a controlled synthesis pathway, enhancing their potential for biomedical and catalytic applications [37, 40, 41].

3.5. FTIR Spectroscopy Analysis. The FTIR results provide information about various functional groups present in the leaf extract, which are used as reducing and stabilizing reagents during the synthesis of A-ZnNPs. The FTIR spectrum of biosynthesized ZnONPs is shown in Figure 5, in which peaks were obtained at 3,397, 2,930, 1,633, 1,408, 1,312, 1,072, 1,025, 821, and 619 cm^{-1}. The peak at 3,397 and 1,408 cm^{-1} was attributed to the stretching vibration for the intramolecular O-H function group and for O-H bending, respectively. The absorption band at 2,930 cm^{-1}, due to C-H stretching in alkane, and a peak at 1,633 cm^{-1}, due to C=O stretching in carboxylic acid, suggest the presence of highly water-soluble phytochemicals adsorbed on the surface of the biosynthesized ZnONPs. The peak at 1,312 gives information about the C-N stretching due to the presence of amine in leaf extract; other peaks at 1,072, 1,025, and 812 cm^{-1} are due to C-O stretching, aromatic C-H in-plane bending, and C=C bending, respectively. However, peaks between 400 and 700 cm^{-1} provide confirmation of the biosynthesis of ZnONPs. The peak at 619 cm^{-1} clearly indicates the presence of Zn-O bond. The FTIR spectra corroborate the role of the phytochemicals of *A. philoxeroides* leaf extract as a reducing and capping reagent for the stability of biosynthesized ZnONPs, which is also confirmed by EDX and dynamic light scattering (DLS) analyses [7, 42–44].

3.6. HRTEM Analysis. The HRTEM images presented in Figure 6(a) and Figure 6(b) confirm the predominantly spherical morphology of the biosynthesized ZnONPs. Particle size analysis using ImageJ software (Figure 6(c)) was based on measurements from 41 nanoparticles, revealing a size distribution ranging from 3.5 to 31.4 nm, with an average particle size of approximately 12 nm. These findings align well with the

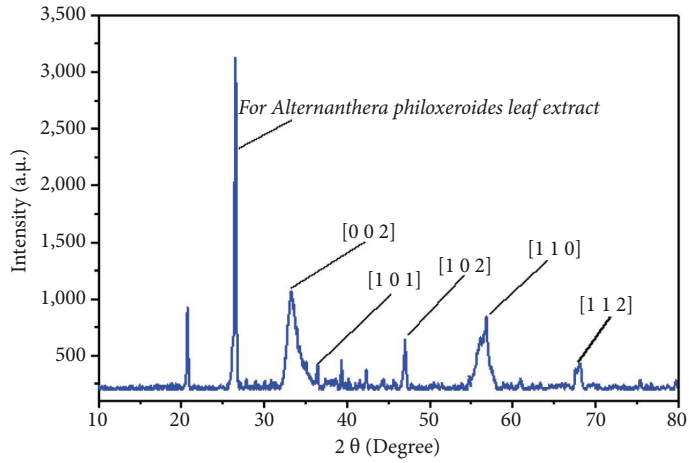


Figure 2: XRD pattern of biosynthesized ZnONPs.

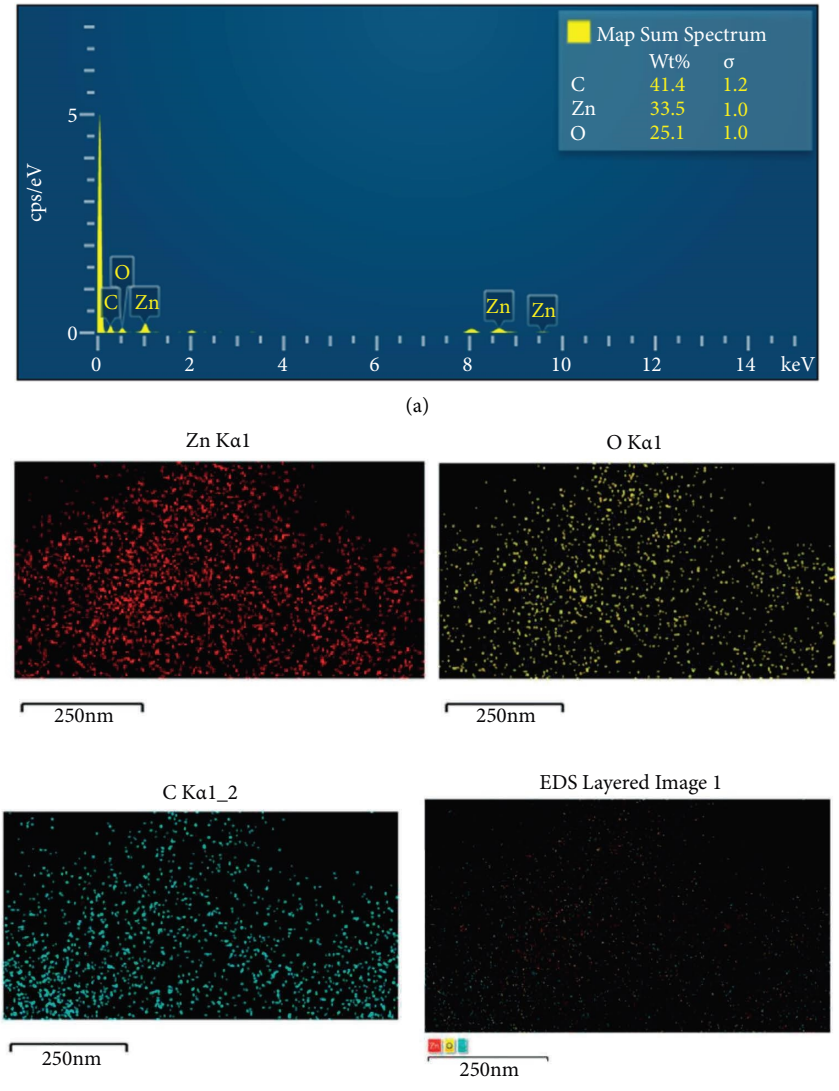


Figure 3: (a) EDX spectra showing the elemental composition of biosynthesized ZnONPs. (b) Elemental mapping of biosynthesized ZnONPs.

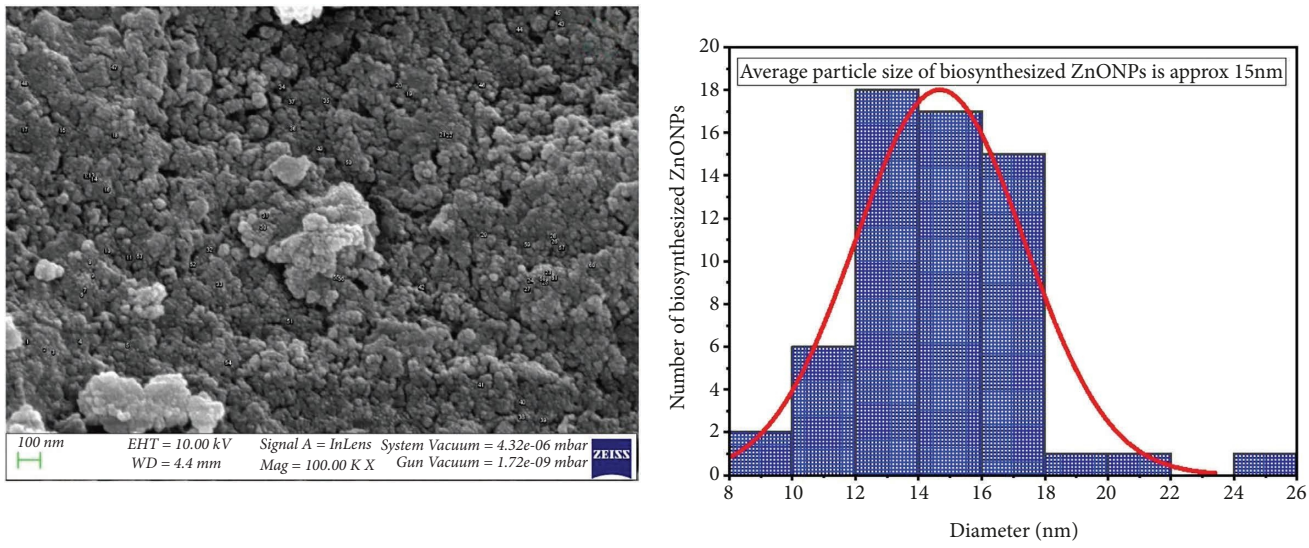


Figure 4: (a) FESEM images of biosynthesized ZnONPs. (b) Particle size distribution of phytochemical-assisted biosynthesized ZnONPs.

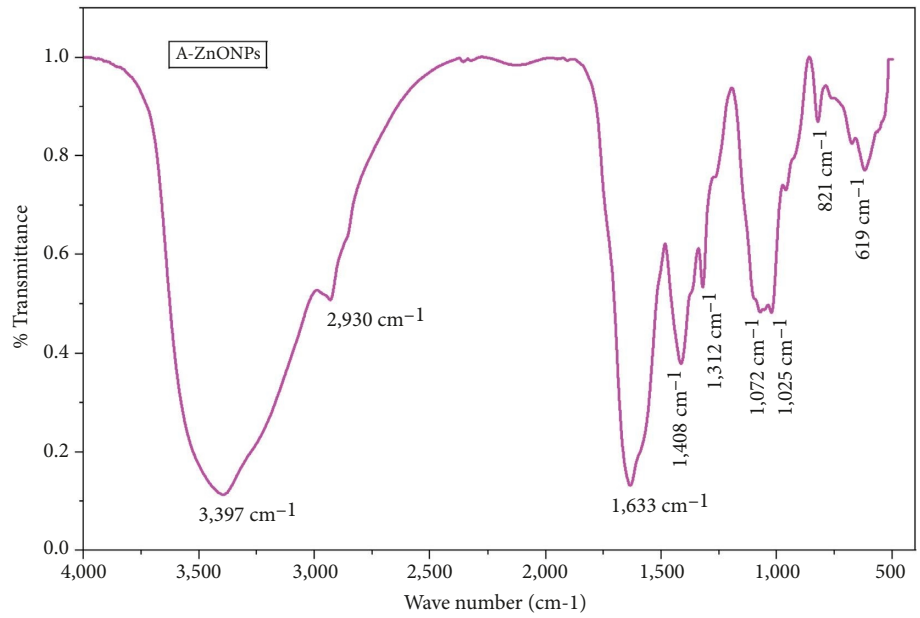


Figure 5: FTIR of biosynthesized A-ZnONPs.

size estimations obtained from XRD and FESEM, reinforcing the reliability of the synthesis method. The SAED pattern in Figure 6(d) displays five concentric diffraction rings, confirming the polycrystalline nature of the ZnONPs. The diffraction rings correspond to the [101], [102], and [110] planes, consistent with the XRD results. This detailed HRTEM analysis not only validates the successful synthesis of well-defined ZnONPs but also emphasizes the structural integrity and crystallinity conferred by the green synthesis approach [45–48].

3.7. DLS Analysis. Figure 7(a) illustrates the particle size distribution of biosynthesized ZnONPs as determined by DLS. Notably, the average particle size observed via DLS is significantly larger than that obtained from HRTEM and FESEM analyses. This discrepancy is attributed to the measurement of hydrodynamic diameter by DLS, which includes the solvation layer surrounding nanoparticles and any possible agglomeration in suspension. The tendency of biosynthesized ZnONPs to aggregate in aqueous media stems from interparticle van der Waals attractions and only moderate electrostatic stabilization. This is further supported by the zeta potential value of −16.4 mV (Figure 7(b)), which suggests limited repulsion between particles, indicating moderate colloidal stability. The negative charge results from phytochemical capping agents derived from the leaf extract, playing a dual role in stabilization and functionalization of the nanoparticle surface. These findings

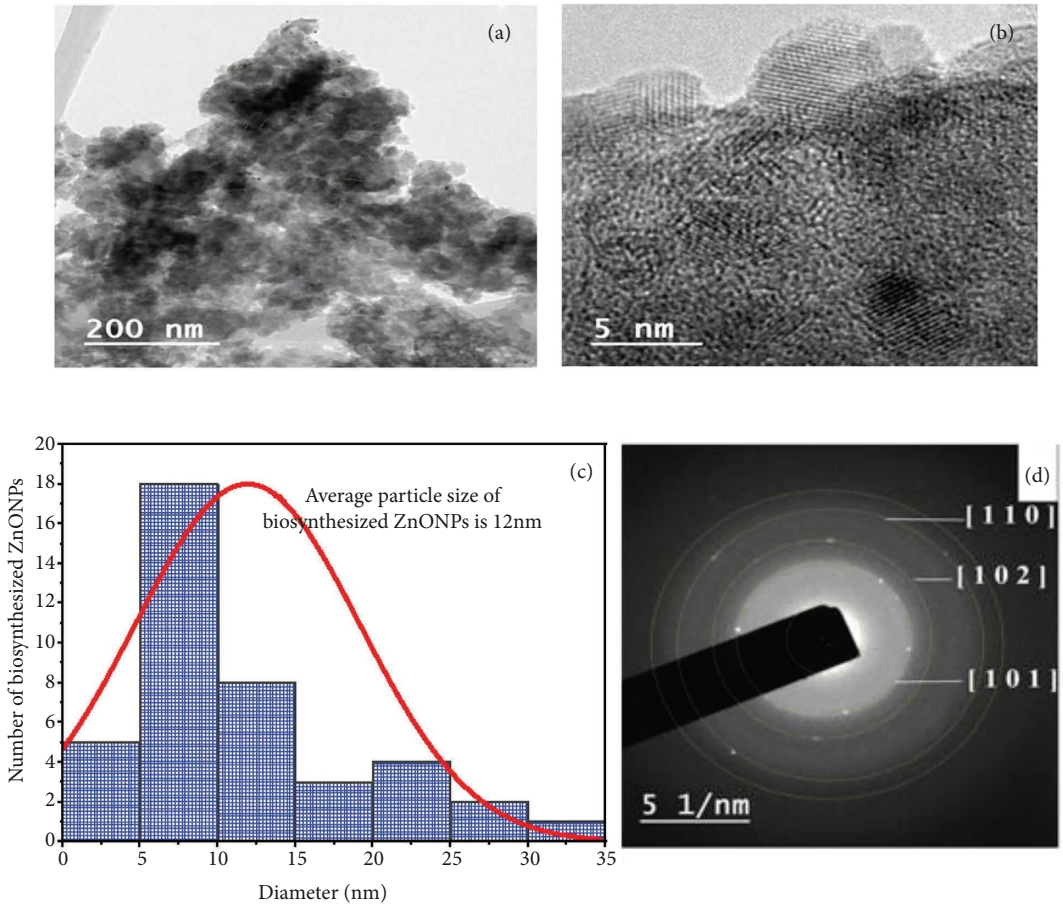
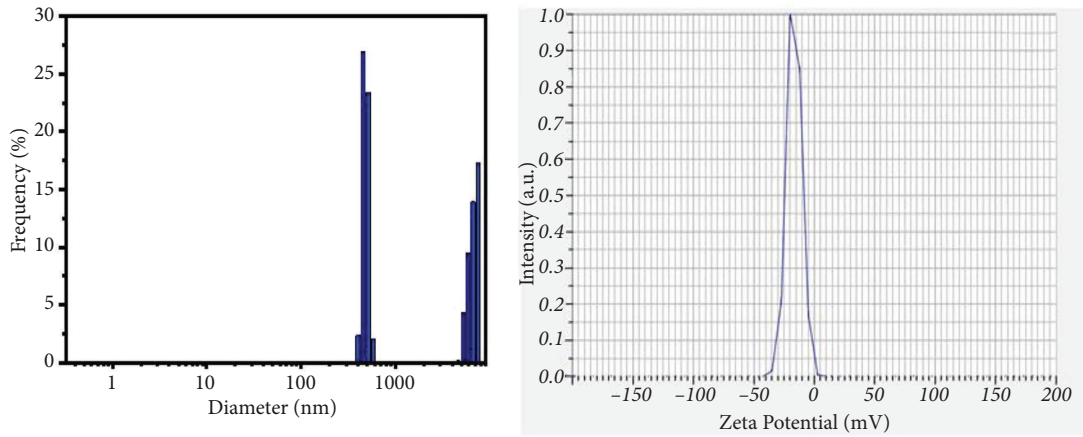


Figure 6: (a, b) HRTEM images of biosynthesized ZnONPs in high and low magnification, (c) particle size distribution of biosynthesized ZnONPs, and (d) SAED patterns of the biosynthesized A-ZnONPs.



(a) (b)

Figure 7: (a) DLS size distribution of biosynthesized ZnONPs. (b) Zeta potential for biosynthesized ZnONPs.

highlight the importance of combining multiple characterization techniques to obtain an accurate understanding of nanoparticle behavior in different environments [22, 49, 50].

3.8. DPPH Assay Analysis. The antioxidant activity of phytochemical-assisted biosynthesized ZnONPs was determined using the DPPH method. In this method, methanol

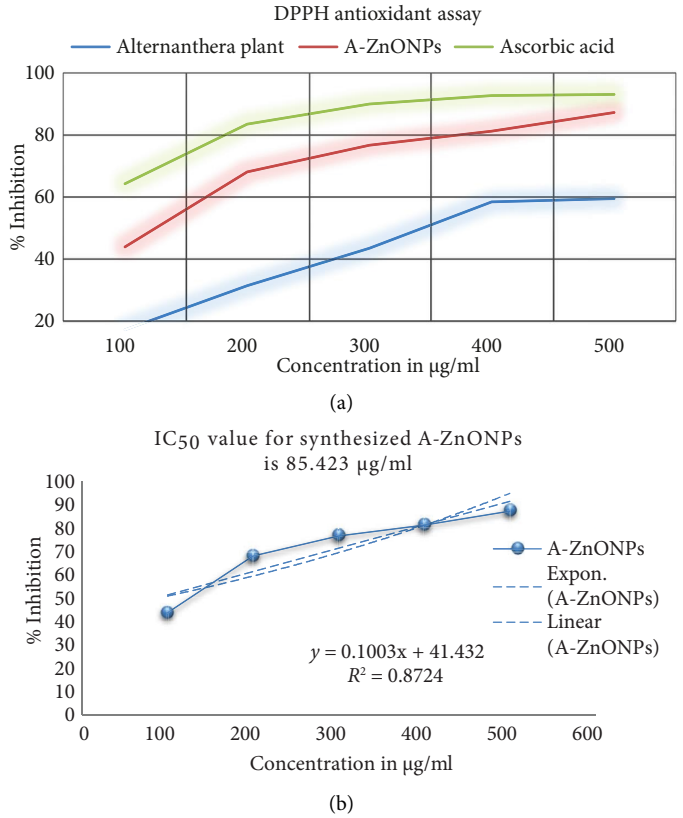


Figure 8: (a) Comparative study of DPPH–free radical scavenging activity for ascorbic acid, leaf extract, and biosynthesized ZnONPs. (b) IC50 value for biosynthesized ZnONPs.

Table 1: IC_{50} value comparison with other ZnONPs.

Plant	Nanoparticles	IC_{50} against DPPH	Reference
Tabernaemontana heyneana Wall. (Leaf)	ZnO	752.30 µg/mL (larger than IC_{50} of biosynthesized ZnONPs)	[53]
Polystichum lentum	ZnO	83.79 µg/mL (nearly similar to IC_{50} biosynthesized ZnONPs)	[54]
Ailanthus altissima leaf	ZnO	78.32 µg/mL (nearly similar to IC_{50} biosynthesized ZnONPs)	[51]
Canthium dicoccum (L.)	ZnO	32.85 µg/mL (less than IC_{50} biosynthesized ZnONPs)	[52]

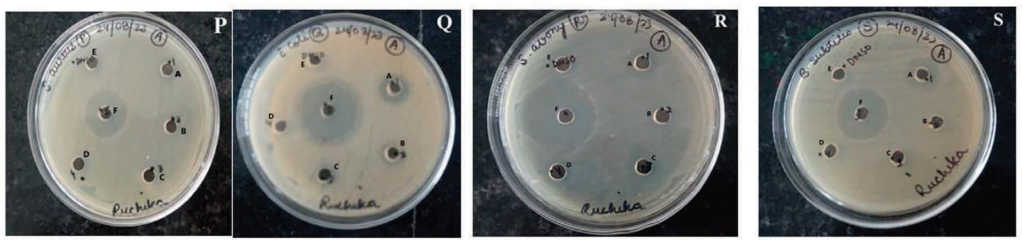


Figure 9: (P) Against *Staphylococcus aureus*, (Q) against *Escherichia coli*, (R) against *Salmonella abony*, and (S) against *Bacillus subtilis*. Inhibition zone of *Alternanthera philoxeroides* extract for different bacteria.

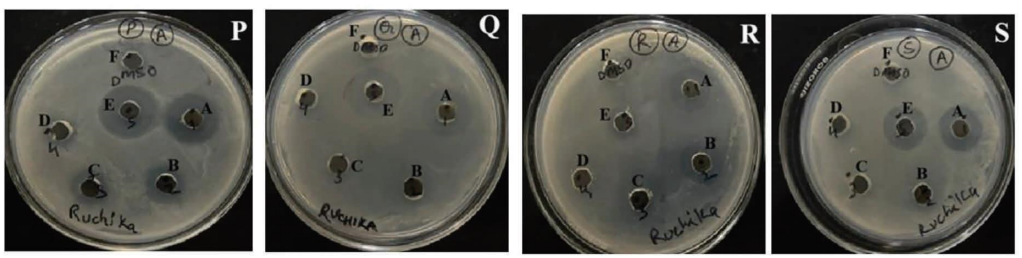


Figure 10: (P) Against *Staphylococcus aureus*, (Q) against *Escherichia coli*, (R) against *Salmonella abony*, and (S) against *Bacillus subtilis*. Inhibition zone of biosynthesized ZnONPs for different bacteria.

Table 2: Inhibition zone diameter (mm) for different bacteria (each type of strain was based on three biological replicates).

Concentration	*Staphylococcus aureus (P)*		*Escherichia coli (Q)*		*Salmonella abony (R)*		*Bacillus subtilis (S)*	
	***Alternanthera philoxeroides* leaf extract**	**Biosynthesized ZnONPs**	***Alternanthera philoxeroides* leaf extract**	**Biosynthesized ZnONPs**	***Alternanthera philoxeroides* leaf extract**	**Biosynthesized ZnONPs**	***Alternanthera philoxeroides* leaf extract**	**Biosynthesized ZnONPs**
2000 μg/mL (A)	5.88 ± 0.28 mm	20.00 ± 0.50 mm	9.66 ± 0.57 mm	24.66 ± 0.57 mm	9.66 ± 0.57 mm	17 ± 1 mm	15.5 ± 0.5 mm	20.33 ± 0.57 mm
1000 μg/mL (B)	4.50 ± 0.50 mm	10.83 ± 0.76 mm	5.83 ± 0.76 mm	19 ± 1 mm	4.33 ± 0.28 mm	11.83 ± 0.28 mm	5.66 ± 0.57 mm	15.66 ± 0.76 mm
500 μg/mL (C)	—	4.5 ± 0.5 mm	—	10.83 ± 0.29 mm	—	7.66 ± 0.28 mm	—	11.83 ± 0.28 mm
250 μg/mL (D)	—	—	—	6.0 ± 0.5 mm	—	—	—	9.16 ± 1.04 mm
Streptomycin μg/mL (F) (positive control)	19.33 ± 0.57 mm	22.83 ± 0.57 mm	24.0 ± 0.5 mm	28.33 ± 0.58 mm	20.33 ± 0.57 mm	21.00 ± 0.86 mm	19.83 ± 0.76 mm	23.16 ± 0.28 mm
DMSO (negative control)	—	—	—	—	—	—	—	—

was used as a solvent, and DPPH was used as a free radical, which gave a violet color to methanol. In the presence of an alcoholic solution of leaf extract and biosynthesized ZnONPs, the violet color of DPPH becomes faint. If the antioxidant property is high, then it changes to yellow after 30 min. Firstly, a prepared alcoholic solution of ascorbic acid, leaf extract, and biosynthesized ZnONPs of different concentrations (100, 200, 300, 400, and 500 μg/mL) is prepared. An equal quantity of DPPH is then added to it for the same duration. Due to the high sensitivity of DPPH toward light, work with DPPH was done in the dark. The percentage inhibition of DPPH for ascorbic acid, leaf extract, and biosynthesized ZnONPs at different concentrations is shown in Figure 8 (a). The percentage inhibition for biosynthesized ZnONPs were 43.88 and 87.36 at concentrations of 100 and 500 μg/mL, respectively; however, for *A. philoxeroides* leaf extract, the values of inhibition percentages for similar concentrations were 17.05 and 59.50, which are less than those of biosynthesized ZnONPs. The result clearly reveals the antioxidant properties of biosynthesized ZnONPs that depend on concentration. On increasing concentration, antioxidant activity increases. Biosynthesized ZnONPs show lower antioxidant activity than standard ascorbic acid but higher than *A. philoxeroides* leaf extract.

The amount of a sample needed to eradicate 50% of free radicals (DPPH) is indicated by the IC_{50} value. A lower IC_{50} value indicates better antioxidant activity against DPPH free radicals. Our results showed that the *A. philoxeroides* leaf extract had an IC_{50} value of 371.8 μg/mL, which is significantly higher than the biosynthesized ZnONPs, with an IC_{50} value of 85.42 μg/mL, as shown in Figure 8(b). This means that biosynthesized ZnONPs have better antioxidant properties than *A. philoxeroides* leaf extract. In comparison, other studies found varying IC_{50} values for ZnONPs made with different leaf extracts. The ZnONPs are made with *Tabernaemontana heyneana Wall.* leaf extract had a much higher IC_{50} value than biosynthesized ZnONPs. On the other hand, the ZnONPs made with *Polystichum lentum* and *Ailanthus altissima leaf* extract had similar IC_{50} values to biosynthesized ZnONPs. Interestingly, the ZnONPs made with *Canthium dicoccum (L.)* extract had a much lower IC_{50} value than biosynthesized ZnONPs, as shown in Table 1, indicating even better antioxidant properties [51–54].

3.9. Antibacterial Activity. Using two Gram-positive and two Gram-negative bacteria, the well disk diffusion method was used to examine the antibacterial potential of produced biosynthesized ZnONPs. Significant zones of inhibition were found for *A. philoxeroides*–derived ZnONPs. The ZOI area is completely concentration-dependent; the ZOI increases with an increase in concentration. The ZOI also depends on size and shape; the possible mechanism behind inhibition of growth could be the formation of ROS, interaction of biosynthesized ZnONPs with proteins, role in DNA replication, and cell wall leakage. ZOI for biosynthesized ZnONPs was also more than 250 μg/mL at 2,000 μg/mL for all bacteria, as shown in Figures 9 and 10. The zone of inhibition for biosynthesized ZnONPs was found to be higher than that for *A. philoxeroides* leaf extract, which indicates that the antibacterial activity of biosynthesized ZnONPs is higher for all the tested bacteria, even at lower concentrations. All the obtained results are given in Table 2. The inhibition zone is shown as $x \pm y$, where x is the average value of the inhibition zone for three replicas, while y is the standard deviation. From the present study, it is observed that Gram-positive and Gram-negative microbes are equally sensitive toward biosynthesized ZnONPs. The highest zone of inhibition, 26 mm, was observed for *S. aureus* at 2000 μg/mL. However, a lower zone of inhibition was observed for *B. subtilis*. These findings are in good agreement with those of reported studies against different pathogens [31, 55–57].

4. Conclusion

This study demonstrates an eco-friendly, simple, and cost-effective approach to synthesizing ZnONPs using *A. philoxeroides* leaf extract, aligning with the principles of green chemistry. The phytochemicals in the leaf extract act as natural capping and reducing agents, eliminating the need for hazardous chemicals or additional stabilizers during the nanoparticle synthesis process. This method offers a safer and more appealing alternative to microbial synthesis techniques. Characterization techniques such as DLS, XRD, FTIR, HRTEM, EDX, and FESEM confirmed the successful synthesis of ZnONPs with an average particle size of 12 nm. These nanoparticles exhibited significantly enhanced antioxidant and antibacterial activities compared to the raw leaf extract, underscoring their potential applications. To further validate these findings, in vivo testing is necessary to explore practical applications, paving the way for environmentally sustainable nanoparticle synthesis. Additionally, this method holds promise for extending green chemistry approaches to the synthesis of other metal nanoparticles.

Nomenclature

Biosynthesized ZnONPs	ZnONPs mediated by *A.* philoxeroides extract
ZnONPs	Zinc oxide nanoparticles
mM	Millimolar
mL	Milliliter
DLS	Dynamic light scattering
DPPH	DPPH: 2,2-diphenyl-1-picrylhydrazyl
JCPDS	Joint committee on powder diffraction standards
FTIR	Fourier transform infrared
DMSO	Dimethyl sulfoxide
UV-Vis	Ultraviolet-visible
FESEM	Field emission scanning electron microscopy
SPR	Surface plasmon resonance
XRD	X-ray beam diffraction
EDX	Energy dispersive X-ray
HRTEM	High-resolution transmission electron microscopy
SAED	Selected area electron diffraction.

Data Availability Statement

The datasets generated and/or analyzed during this study are available within this paper.

Ethics Statement

This research was conducted in a legal and ethical way and is completely in compliance with ethical standards.

Disclosure

All authors have read and agreed to the published version of the manuscript and all authors agree to be accountable for the research presented.

Conflicts of Interest

The authors declare no conflicts of interest.

Author Contributions

Ruchika Sharma contributed to the methodology and formal analysis. Rakesh Kumar Bachheti and Archana Bachheti contributed as writing–original draft drafted. Limenew Abate Worku and Sheetal Tyagi as supervision of the experimental work as well as paper writing and providing guidance throughout the process.

Funding

There is no external funding to do this research work.

References

[1] M. Shaaban and A. M. El-Mahdy, "Biosynthesis of Ag, Se, and ZnO Nanoparticles with Antimicrobial Activities Against Resistant Pathogens Using Waste Isolate Streptomyces enissocaesilis," *IET Nanobiotechnology* 12, no. 6 (2018): 741–747, https://doi.org/10.1049/iet-nbt.2017.0213.

[2] H. Agarwal, S. Venkat Kumar, and S. Rajeshkumar, "A Review on Green Synthesis of Zinc Oxide nanoparticles–An Eco-Friendly Approach," *Resource-Efficient Technologies* 3, no. 4 (2017): 406–413, https://doi.org/10.1016/j.reffit.2017.03.002.

[3] P. Basnet, T. Inakhunbi Chanu, D. Samanta, and S. Chatterjee, "A Review on bio-synthesized Zinc Oxide Nanoparticles Using Plant Extracts as Reductants and Stabilizing Agents," *Journal of Photochemistry and Photobiology B: Biology* 183 (2018): 201–221, https://doi.org/10.1016/j.jphotobiol.2018.04.036.

[4] S. S. Salem and A. Fouda, "Green Synthesis of Metallic Nanoparticles and their Prospective Biotechnological Applications: an Overview," *Biological Trace Element Research* 199, no. 1 (2021): 344–370, https://doi.org/10.1007/s12011-020-02138-3.

[5] G. Karunakaran, K. G. Sudha, S. Ali, and E.-B. Cho, "Biosynthesis of Nanoparticles from Various Biological Sources and its Biomedical Applications," *Molecules* 28, no. 11 (2023): 4527, https://doi.org/10.3390/molecules28114527.

[6] C. Pandit, A. Roy, S. Ghotekar, et al., "Biological Agents for Synthesis of Nanoparticles and their Applications," *Journal of King Saud University Science* 34, no. 3 (2022): 101869, https://doi.org/10.1016/j.jksus.2022.101869.

[7] A. M. Abdo, A. Fouda, A. M. Eid, et al., "Green Synthesis of Zinc Oxide Nanoparticles (ZnO-NPs) by *Pseudomonas aeruginosa* and Their Activity Against Pathogenic Microbes and Common House Mosquito, *Culex pipiens*," *Materials* 14, no. 22 (2021): 6983, https://doi.org/10.3390/ma14226983.

[8] M. A. Ali, T. Ahmed, W. Wu, et al., "Advancements in Plant and Microbe-Based Synthesis of Metallic Nanoparticles and their Antimicrobial Activity Against Plant Pathogens," *Nanomaterials* 10, no. 6 (2020): 1146, https://doi.org/10.3390/nano10061146.

[9] D. Haritha, M. Faiz Ahmed, S. Bala, and D. Choudhury, "Eco-Friendly Plant Based on Botanical Pesticides," *Plant archives* 21, no. Suppliment-1 (2021): 2197–2204, https://doi.org/10.51470/plantarchives.2021.v21.s1.362.

[10] J. O. Adeyemi, A. O. Oriola, D. C. Onwudiwe, and A. O. Oyedeji, "Plant Extracts Mediated Metal-based Nanoparticles: Synthesis and Biological Applications," *Biomolecules* 12, no. 5 (2022): 627, https://doi.org/10.3390/biom12050627.

[11] R. Sharma, P. Janmeda, P. Chaudhary, and S. Rawat, "Antipyretic Medicinal Plants, Phytocompounds, and Green Nanoparticles: an Updated Review," *Current Pharmaceutical Biotechnology* 24, no. 1 (2023): 23–49, https://doi.org/10.2174/1389201023666220330005020.

[12] P. Monika, M. Chandraprabha, R. Hari Krishna, et al., "Recent Advances in Pomegranate Peel Extract Mediated Nanoparticles for Clinical and Biomedical Applications," *Biotechnology & Genetic Engineering Reviews* 40, no. 4 (2024): 3379–3407, https://doi.org/10.1080/02648725.2022.2122299.

[13] P. Prete, N. Lovergine, and L. Tapfer, "Nanostructure Size Evolution During Au-catalysed Growth by carbo-thermal Evaporation of well-aligned ZnO Nanowires on (100) Si," *Applied Physics A* 88, no. 1 (2007): 21–26, https://doi.org/10.1007/s00339-007-3946-4.

[14] S. Thiyyanthiruthy Kumbalaparambil, A. Haridas Chandaparambil, and K. Naskar, "Sustainable ZnO Nanoparticles Using Sweet Lime Peel Extract: Eco-Friendly Activator in Rubber for Tire Applications," *Express Polymer Letters* 18, no. 10 (2024): 991–1007, https://doi.org/10.3144/expresspolymlett.2024.76.

[15] A. Rani, N. Kumar, and M. Kumar, *Environmentally Friendly Green Approaches and Applications of Nanoparticles, Metal Oxide–Based Carbon Nanocomposites for Environmental Remediation and Safety* (CRC Press (a subsidiary of Taylor & Francis Group), 2023).

[16] S. Tabrez, A. U. Khan, M. Hoque, M. Suhail, M. I. Khan, and T. A. Zughaibi, "Biosynthesis of ZnO NPs from Pumpkin Seeds' Extract and Elucidation of its Anticancer Potential Against Breast Cancer," *Nanotechnology Reviews* 11, no. 1 (2022): 2714–2725, https://doi.org/10.1515/ntrev-2022-0154.

[17] S. Ahmad, M. Usman, M. Hashim, A. Ali, R. Shah, and N. U. Rahman, "Investigation of Optical and Dielectric Properties of Nickel-Doped Zinc Oxide Nanostructures Prepared via Coprecipitation Method," *Nanomaterials and Nanotechnology* 2024, no. 1 (2024): 1–11, https://doi.org/10.1155/2024/8330886.

[18] R. Prakash, "Medicinal Plants Used by Tribal Communities: a Study of Uttarakhand Himalayan Region," *International Journal of Humanities and Social Science Invention* 4 (2015): 55–61.

[19] A. Singh, M. C. Nautiyal, R. M. Kunwar, and R. W. Bussmann, "Ethnomedicinal Plants Used by Local Inhabitants of Jakholi Block, Rudraprayag District, Western Himalaya, India," *Journal of Ethnobiology and Ethnomedicine* 13 (2017): 49, https://doi.org/10.1186/s13002-017-0178-3.

[20] U. A. Pamila and S. Karpagam, "A Comparative Study on Phytoconsti-Tuents of Three Different Species of Genus Alternanthera," *Int J Innov Res Adv Stud* 5 (2018): 52–54.

[21] R. Sharma, S. Tyagi, A. Kandwal, R. Bachheti, and A. Bachheti, "Green Synthesis of Silver/Silver Chloride Nanoparticles Mediated by Alternanthera philoxeroides Leaf Extract and Their Biological Activity," *Russian Journal of General Chemistry* 94, no. 7 (2024): 1750–1757, https://doi.org/10.1134/s1070363224070181.

[22] S. K. Chaudhuri and L. Malodia, "Biosynthesis of Zinc Oxide Nanoparticles Using Leaf Extract of Calotropis Gigantea: Characterization and its Evaluation on Tree Seedling Growth in Nursery Stage," *Applied Nanoscience* 7, no. 8 (2017): 501–512, https://doi.org/10.1007/s13204-017-0586-7.

[23] S. Chinnappan, S. Kandasamy, S. Arumugam, K.-K. Seralathan, S. Thangaswamy, and G. Muthusamy, "Biomimetic Synthesis of Silver Nanoparticles Using Flower Extract of Bauhinia purpurea and its Antibacterial Activity Against Clinical Pathogens," *Environmental Science and Pollution Research* 25, no. 1 (2018): 963–969, https://doi.org/10.1007/s11356-017-0841-1.

[24] M. Nilavukkarasi, S. Vijayakumar, and S. Prathipkumar, "Capparis zeylanica Mediated bio-synthesized ZnO Nanoparticles as Antimicrobial, Photocatalytic and Anti-cancer Applications," *Materials Science for Energy Technologies* 3 (2020): 335–343, https://doi.org/10.1016/j.mset.2019.12.004.

[25] M. T. El-Saadony, G. Fang, S. Yan, et al., "Green Synthesis of Zinc Oxide Nanoparticles: Preparation, Characterization, and Biomedical applications-a Review," *International Journal of Nanomedicine* 19 (2024): 12889–12937, https://doi.org/10.2147/ijn.s487188.

[26] P. Manimegalai, K. Selvam, S. Loganathan, et al., "Green Synthesis of Zinc Oxide (ZnO) Nanoparticles Using Aqueous Leaf Extract of Hardwickia Binata: Their Characterizations and Biological Applications," *Biomass Conversion and Biorefinery* 14, no. 11 (2024): 12559–12574, https://doi.org/10.1007/s13399-023-04279-6.

[27] V. S. Kotakadi, S. A. Gaddam, P. Kotha, R. Allagadda, A. Rao Ch, and S. G. Dvr, "Bio-Inspired Multifunctional Zinc Oxide Nanoparticles by Leaf Extract of Andrographis Serpilifolia and their Enhanced Antioxidant, Antimicrobial, and Antidiabetic Activity—A 3-in-1 System," *Particulate Science and Technology* 40, no. 4 (2022): 485–499, https://doi.org/10.1080/02726351.2021.1966145.

[28] C. Zhao, X. Zhang, and Y. Zheng, "Biosynthesis of Polyphenols Functionalized ZnO Nanoparticles: Characterization and their Effect on Human Pancreatic Cancer Cell Line," *Journal of Photochemistry and Photobiology B: Biology* 183 (2018): 142–146, https://doi.org/10.1016/j.jphotobiol.2018.04.031.

[29] M. Ghareib, M. Abu Tahon, W. E. Abdallah, and M. Hussein, "Free Radical Scavenging Activity of Zinc Oxide Nanoparticles Biosynthesised Using Aspergillus carneus," *Micro & Nano Letters* 14, no. 11 (2019): 1157–1162, https://doi.org/10.1049/mnl.2019.0218.

[30] Z. S. Keskin and U. Açıkel, "Biosynthesis, Characterization and Antioxidant Properties of ZnO Nanoparticles Using Punica granatum Peel Extract as Reducing Agent," *Cumhuriyet Science Journal* 44, no. 1 (2023): 90–98, https://doi.org/10.17776/csj.1223357.

[31] S. Irshad, M. Riaz, A. Anjum, S. Sana, R. Saleem, and A. Shaukat, "Biosynthesis of ZnO Nanoparticles Using Ocimum basilicum and Determination of its Antimicrobial Activity" (2020).

[32] M. H. Kalaba, G. M. El-Sherbiny, E. A. Ewais, O. M. Darwesh, and S. A. Moghannem, "Green Synthesis of Zinc Oxide Nanoparticles (ZnO-NPs) by Streptomyces baarnensis and its Active Metabolite (Ka): a Promising Combination Against multidrug-resistant ESKAPE Pathogens and Cytotoxicity," *BMC Microbiology* 24, no. 1 (2024): 254, https://doi.org/10.1186/s12866-024-03392-4.

[33] G. Sangeetha, S. Rajeshwari, and R. Venckatesh, "Green Synthesis of Zinc Oxide Nanoparticles by Aloe barbadensis Miller Leaf Extract: Structure and Optical Properties," *Materials Research Bulletin* 46, no. 12 (2011): 2560–2566, https://doi.org/10.1016/j.materresbull.2011.07.046.

[34] S. Vijayakumar, S. Mahadevan, P. Arulmozhi, S. Sriram, and P. Praseetha, "Green Synthesis of Zinc Oxide Nanoparticles Using Atalantia monophylla Leaf Extracts: Characterization and Antimicrobial Analysis," *Materials Science in Semiconductor Processing* 82 (2018): 39–45, https://doi.org/10.1016/j.mssp.2018.03.017.

[35] M. Batool, S. Khurshid, Z. Qureshi, and W. M. Daoush, "Adsorption, Antimicrobial and Wound Healing Activities of Biosynthesised Zinc Oxide Nanoparticles," *Chemical Papers* 75, no. 3 (2021): 893–907, https://doi.org/10.1007/s11696-020-01343-7.

[36] M. Hasan, M. Altaf, A. Zafar, et al., "Bioinspired Synthesis of Zinc Oxide nano-flowers: a Surface Enhanced Antibacterial and Harvesting Efficiency," *Materials Science and Engineering: C* 119 (2021): 111280, https://doi.org/10.1016/j.msec.2020.111280.

[37] A. Shamim, T. Mahmood, and M. B. Abid, "Biogenic Synthesis of Zinc Oxide (ZnO) Nanoparticles Using a Fungus (Aspargillus niger) and Their Characterization," *International Journal of Chemistry* 11, no. 2 (2019): 119, https://doi.org/10.5539/ijc.v11n2p119.

[38] V. Katta and R. Dubey, "Green Synthesis of Silver Nanoparticles Using Tagetes erecta Plant and Investigation of their Structural, Optical, Chemical and Morphological Properties," *Materials Today: Proceedings* 45 (2021): 794–798, https://doi.org/10.1016/j.matpr.2020.02.809.

[39] V. Nezamabadi, M. R. Akhgar, B. Tahamipour, and P. Rajaei, "Biosynthesis and Antibacterial Activity of ZnO Nanoparticles by Artemisia aucheri Extract," *Iranian Journal of Biotechnology* 18, no. 2 (2020): e2426, https://doi.org/10.30498/IJB.2020.151379.2426.

[40] D. Manyasree, P. Kiranmayi, and V. R. Kolli, "Characterization and Antibacterial Activity of ZnO Nanoparticles Synthesized by Co-Precipitation Method," *International Journal of Applied Pharmaceutics* 10, no. 6 (2018): 224–228, https://doi.org/10.22159/ijap.2018v10i6.29376.

[41] N. Shah, G. Priyadarshi, B. Patel, et al., "Green Synthesis of ZnO Nanoparticles Using Microbacterium Arborescens: a Multifunctional Approach in Environment, Health, and Agriculture," *Water Reuse* (2025): jwrd2025004.

[42] K. M. Ezealisiji, X. Siwe-Noundou, B. Maduelosi, N. Nwachukwu, and R. W. M. Krause, "Green Synthesis of Zinc Oxide Nanoparticles Using Solanum torvum (L) Leaf Extract and Evaluation of the Toxicological Profile of the ZnO Nanoparticles–Hydrogel Composite in Wistar Albino Rats," *International Nano Letters* 9, no. 2 (2019): 99–107, https://doi.org/10.1007/s40089-018-0263-1.

[43] M. D. Jayappa, C. K. Ramaiah, M. A. P. Kumar, et al., "Green Synthesis of Zinc Oxide Nanoparticles from the Leaf, Stem and in Vitro Grown Callus of *Mussaenda frondosa* L.: Characterization and their Applications," *Applied Nanoscience* 10, no. 8 (2020): 3057–3074, https://doi.org/10.1007/s13204-020-01382-2.

[44] G. Rajivgandhi, B. M. Gnanamangai, T. H. Prabha, et al., "Biosynthesized Zinc Oxide Nanoparticles (ZnO NPs) Using Actinomycetes Enhance the Anti-bacterial Efficacy Against *K. Pneumoniae*," *Journal of King Saud University-Science* 34 (2022): 101731.

[45] M. Chennimalai, J. Y. Do, M. Kang, and T. Senthil, "A Facile Green Approach of ZnO NRs Synthesized via *Ricinus communis* L. Leaf Extract for Biological Activities," *Materials Science and Engineering: C* 103 (2019): 109844, https://doi.org/10.1016/j.msec.2019.109844.

[46] S. Ravichandran, J. Radhakrishnan, P. Sengodan, R. Rajendran, R. Ramalingam, and K. D. Arunachalam, "Bio Synthesis of Zinc Oxide Nanoparticles Using Clerodendrum phlomidis Extract for Antibacterial, Anticancer, Antioxidant and Photocatalytic Studies," *Journal of Materials Science: Materials in Electronics* 33, no. 14 (2022): 11455–11466, https://doi.org/10.1007/s10854-022-08118-8.

[47] F. Thema, E. Manikandan, M. Dhlamini, and M. Maaza, "Green Synthesis of ZnO Nanoparticles via *Agathosma betulina* Natural Extract," *Materials Letters* 161 (2015): 124–127, https://doi.org/10.1016/j.matlet.2015.08.052.

[48] S. Zhou, Y. Qin, A. Lei, et al., "The Role of Green Synthesis Metal and Metal Oxide Nanoparticles in Oral Cancer Therapy: a Review," *Journal of Drug Targeting* 33, no. 6 (2025): 853–876, https://doi.org/10.1080/1061186x.2025.2461091.

[49] T. M. Abdelghany, A. M. Al-Rajhi, R. Yahya, et al., "Phytofabrication of Zinc Oxide Nanoparticles with Advanced Characterization and its Antioxidant, Anticancer, and Antimicrobial Activity Against Pathogenic Microorganisms," *Biomass Conversion and Biorefinery* 13, no. 1 (2023): 417–430, https://doi.org/10.1007/s13399-022-03412-1.

[50] J. González-Fernández, D. David Pinzón-Moreno, A. Alexander Neciosup-Puican, and M. Verónica Carranza-Oropeza, "Green Method, Optical and Structural Characterization of ZnO Nanoparticles Synthesized Using Leaves Extract of M. oleifera," *Journal of Renewable Materials* 10, no. 3 (2022): 833–847, https://doi.org/10.32604/jrm.2022.017377.

[51] S. Shabbir Awan, R. Taj Khan, A. Mehmood, et al., "Ailanthus altissima Leaf Extract Mediated Green Production of Zinc Oxide (ZnO) Nanoparticles for Antibacterial and Antioxidant Activity," *Saudi Journal of Biological Sciences* 30, no. 1 (2023): 103487, https://doi.org/10.1016/j.sjbs.2022.103487.

[52] C. Mahendra, M. N. Chandra, M. Murali, et al., "Phyto-Fabricated ZnO Nanoparticles from Canthium Dicoccum (L.) for Antimicrobial, Anti-tuberculosis and Antioxidant Activity," *Process Biochemistry* 89 (2020): 220–226, https://doi.org/10.1016/j.procbio.2019.10.020.

[53] D. Manasa, K. Chandrashekar, M. A. Pavan Kumar, et al., "Proficient Synthesis of Zinc Oxide Nanoparticles from Tabernaemontana heyneana Wall. via Green Combustion Method: Antioxidant, Anti-Inflammatory, Antidiabetic, Anticancer and Photocatalytic Activities," *Results in Chemistry* 3 (2021): 100178, https://doi.org/10.1016/j.rechem.2021.100178.

[54] D. K. Shrestha, A. B. Magar, M. Bhusal, et al., "Synthesis of Silver and Zinc Oxide Nanoparticles Using Polystichum lentum Extract for the Potential Antibacterial, Antioxidant, and Anticancer Activities," *Journal of Chemistry* 2024, no. 1 (2024): 1876560, https://doi.org/10.1155/2024/1876560.

[55] M. A. Ansari, H. M. Khan, A. A. Khan, A. Sultan, and A. Azam, "Synthesis and Characterization of the Antibacterial Potential of ZnO Nanoparticles Against extended-spectrum β-lactamases-producing *Escherichia coli* and *Klebsiella pneumoniae* Isolated from a Tertiary Care Hospital of North India," *Applied Microbiology and Biotechnology* 94, no. 2 (2012): 467–477, https://doi.org/10.1007/s00253-011-3733-1.

[56] A. A. El-Fallal, R. A. Elfayoumy, and M. M. El-Zahed, "Antibacterial Activity of Biosynthesized Zinc Oxide Nanoparticles Using Kombucha Extract," *SN Applied Sciences* 5, no. 12 (2023): 332, https://doi.org/10.1007/s42452-023-05546-x.

[57] S. Senthilkumar and T. Sivakumar, "Green Tea (Camellia sinensis) Mediated Synthesis of Zinc Oxide (ZnO) Nanoparticles and Studies on their Antimicrobial Activities," *Int. J. Pharm. Sci* 6 (2014): 461–465.